



HAL
open science

New description of fluidization regimes

Régis Andreux, Thierry Gauthier, Jamal Chaouki, Olivier Simonin

► **To cite this version:**

Régis Andreux, Thierry Gauthier, Jamal Chaouki, Olivier Simonin. New description of fluidization regimes. *AICHE Journal*, 2005, 51 (4), pp.1125-1130. 10.1002/aic.10380 . hal-00467486

HAL Id: hal-00467486

<https://hal.science/hal-00467486>

Submitted on 17 Oct 2023

HAL is a multi-disciplinary open access archive for the deposit and dissemination of scientific research documents, whether they are published or not. The documents may come from teaching and research institutions in France or abroad, or from public or private research centers.

L'archive ouverte pluridisciplinaire **HAL**, est destinée au dépôt et à la diffusion de documents scientifiques de niveau recherche, publiés ou non, émanant des établissements d'enseignement et de recherche français ou étrangers, des laboratoires publics ou privés.

A NEW DESCRIPTION OF FLUIDIZATION REGIMES

R. Andreux^{1*}, J. Chaouki², T. Gauthier¹, O. Simonin³

1. Institut Français du Pétrole, Centre d'Etudes et de Développements Industriels, Solaize B.P.3, 69390 Vernaison , France
2. Ecole Polytechnique de Montréal, Chemical Engineering Dpt., C.P. 6079, succ. Centre-ville, Montréal, Quebec, Canada H3C 3A7
3. Institut de Mécanique des Fluides de Toulouse, UMR CNRS/INPT/UPS 5502, Allée du Pr. Soula, 31400, Toulouse, France

ABSTRACT

Two pressure probes and an intrusive bi-optical probe provide experimental data in the bubbling and turbulent regimes to improve our understanding of the bubbling to fast fluidization regimes transition. Pressure, voidage and bubbling properties assessment allows for new description of turbulent fluidization hydrodynamics. Appreciable changes in the hydrodynamics appear well below the transition criterion U_c determined based on pressure fluctuations: bubbles are fast bubbles below U_c , in bubble-emulsion equilibrium state at U_c , and then become slow bubbles for higher fluidizing velocity; the maximum of the total fluidizing gas fraction in the bubble-phase is reached below U_c and never exceeds 75-80 %. The fluidizing velocity at which major hydrodynamics modifications are observed is lower than U_c . This critical velocity is detected with pressure drop

assessment or voidage fluctuations frequency analysis. Moreover, it can be theoretically calculated from the two-phase modeling correlations supplemented with a new criterion deduced from our experiments.

TOPICAL HEADING:

Particle Technology and Fluidization

KEY WORDS:

Experiments – Optical probe – Transition – Bubbling regime – Turbulent regime

INTRODUCTION

What is occurring in the turbulent fluidization regime? Since Lanneau¹, this regime has been widely investigated over the years and is today considered to be the transition between bubbling and fast fluidization, beginning at the gas velocity transition criterion U_c . However, its hydrodynamics is still not well understood and controversy remains about what it really is. Misunderstanding is reinforced by the transition criterion U_c , found to be very dependent on the measurement technique, static bed height, column diameter, particle size distribution, temperature, pressure, etc. The turbulent fluidization regime is nowadays alternately understood and modeled as a peculiar regime with sharp beginning and ending transitions, or as a combination of features which pertains to different fluidization regimes. One should refer to the publications of Horio et al.², Rhodes³ and Bi et al.⁴ for reviews of gas-solid turbulent fluidization and the questions raised.

Understanding the turbulent fluidization requires knowledge of the transition criterion, voidages, bubble size and velocity, hold-up, instantaneous bubble shape, and local interstitial gas velocity. However, previous experimental studies have always been restricted on the bubbling property or the solid behavior assessments to describe or confirm the different fluidization regimes : pressure drop fluctuation measurements still are the more common experimental techniques for analyzing the regime transition (Tannous et al.⁵ ; Bai et al.⁶) ; the non-intrusive electrical capacitance tomography technique has been recently used to show that U_c determined based on standard deviation, amplitude and solid fraction distribution analysis coincide (Makkawi and Wright⁷) ; the optical probe technique has sometimes been used to describe the fluidization regimes based on the description of the bubbling regimes (Svensson et al.⁸) ; finally, visual observations have always provided interesting descriptions of the bubbling phenomena through the whole fluidization regimes (Yamazaki et al.⁹ ; Zijerveld et al.¹⁰).

We are convinced that the study of the interstitial gas in the emulsion-phase is as relevant as the bed property measurements to understand the fluidization regimes. Then, pressure drop probes and bi-optical probes are used to assess full instantaneous and averaged bed behaviors. Mass and momentum balances are then performed to assess non measurable data to carry the analysis to its conclusion. Thus, the velocity transition criterion U_c will be found not to be the only critical parameter in the bubbling to fast fluidization regimes.

The aims of the present work are, then, (i) to establish an extensive data base of experimental results in gas-solid bubbling and turbulent regimes (ii) to measure peculiar variables in the whole transition regime (iii) to describe nowadays unknown trends in the bubbling to fast fluidization regimes.

EXPERIMENTAL PROCEDURE

The experiments were carried out in a transparent cold air-fluidized bed 152 mm in diameter and 1.5 m high with solids returned to freeboard region. Air ($\rho_1=1.2 \text{ kg/m}^3$, $\mu_1=1.8 \cdot 10^{-5} \text{ Pa}\cdot\text{s}$) was introduced through a nozzle type distributor placed above a porous plate providing high pressure drop. Typical sand particles ($\rho_2=2585 \pm 35 \text{ kg/m}^3$, $d_p = 1/\sum(x_i/d_i) = 250 \text{ }\mu\text{m}$, $\varepsilon_{mf} = 44 \%$) are fluidized between 0.12 and 1.50 m/s. The static height of the bed is 30 cm.

The local instantaneous pressure drop between 25 and 35 cm above the distributor is provided by two sensors connected to pressure taps with 4 mm internal diameter pipes, following Xie and Geldart¹¹. Data are acquired with a sampling frequency of 20 Hz. The transition criterion U_c is determined based on the standard deviation of the pressure fluctuations.

The local instantaneous hydrodynamics were measured at 30 cm above the distributor with a bi-optical probe 3 mm in diameter. The two measurement volumes were 1 mm^3 and 1.8 mm apart. Data are acquired with a sampling frequency of 15630 Hz over 202 s. Voidages are obtained with a preliminary calibration of the optical signals provided by the probe. Bubble- and emulsion- phases are discriminated with the upper threshold voidage, ε_{th} , defined as the minimum of the PDF of the local voidage, ε_f (Cui et al.¹²). Bubble chord and velocity are calculated with intercorrelation between the two signals given by the probe (Bayle et al.¹³). The local instantaneous bubble hold-up is calculated as $\delta = (\varepsilon_f - \varepsilon_e) / (\varepsilon_b - \varepsilon_e)$ using the local instantaneous bubble- and emulsion- phase, and

bed voidages. Mean values are obtained by arithmetic averaging. The bubbling frequency is defined as the number of bubbles detected during the sampling time, reported to one second. The dominant frequency of the local voidage is given by FFT treatment combined with optimized mobile-averaging filtering.

RESULTS AND DISCUSSION

Bubbling to turbulent regime transition

The transition criterion U_c determined based on pressure fluctuations is equal to $U_c = 0.85$ m/s (Fig. 1). It agrees with Gonzalez¹⁴'s, Bi and Grace¹⁵ and Abba¹⁶'s correlations.

Hydrodynamics properties

Time-averaged voidage calculated with the local pressure drop is consistent with that of the literature (Fig. 2): it strongly increases at low fluidizing velocity and is nearly constant in the bubbling to turbulent regime transition (Lancia et al.¹⁷). Break-up in the experimental curve appears at a fluidizing velocity $U_{c'}$, 0.45 m/s, lower than U_c . It is not caused by a sudden change in the global bed structure, as core-annulus appearing or gas by-passing: the time-averaged radial profile of the local voidage keeps its flat shape when increasing the fluidizing velocity (Fig. 3). It may be the resulting effect of the modification of the local bed structure, characterized by a decreasing in the emulsion phase predominance of the probability density function of local voidage (Fig. 4) and a maximum in the dominant frequency of the voidage time-fluctuations (Fig. 5). These trends are discussed below. No change in the fluidized bed behaviors is observed at U_c .

Bubbling properties

The upper threshold voidage ε_{th} is nearly constant on most of the whole fluidizing velocity range (Fig. 6). The emulsion-phase voidage, ε_e , increases with the fluidizing velocity concurring with the classic description of the turbulent fluidization regime, while the bubble-phase, not free of particle, begins more and more diluted. But, roughly, the emulsion- and bubble- phases voidages remain constant when the fluidizing velocity is higher than U_c , 70 % and 95 % respectively. This agrees with previous experiments of Cui et al.¹⁸ under similar operating conditions

The measured mean bubble chord, d_b , is consistent with the value from the correlation of Darton et al.¹⁹ obtained in the formalism of the two-phase modeling (Fig. 7) :

$$d_b = \frac{0.54(U - U_{mf})^{0.4} \left(z + 4\sqrt{5.52 \times 10^{-5}} \right)^{0.8}}{g^{0.2}} .$$

The same approach, using Davidson-Harrison²⁰'s correlation, $U_b = U - U_{mf} + 0.711\sqrt{gd_b}$ (U_{mf} given by either Ergun²¹'s or Grace²²'s correlation), gives acceptable estimation of the bubble velocity, U_b , when the fluidizing velocity ranges between U_{mf} and U_c . (Fig. 8). However, it leads to slanted estimations for higher fluidizing velocities, and predictions are up to a factor of two from the experimental data.

Void-phase fractions, δ , are compared to the Davidson-Harrison's correlation which follows from the assumptions of empty bubbles and superficial gas velocity in the emulsion equal to U_{mf} : $\delta = (U - U_{mf})/U_b$, U_b given by the model (Fig. 9).

Surprisingly, the model predictions fit well the experimental data even though (i) bubbles are considered free of particles (ii) bubble velocity values are overestimated.

Extra data assessments

Considering Davidson-Harrison's correlations, the superficial gas velocity in the emulsion phase, U_{1e} , must be greater than U_{mf} when the fluidizing velocity is higher than U_c , in order to cancel their wrong assumptions out. Combining the experimental results of ε_f , ε_e , ε_b , U_b , and δ , one can estimate U_{1e} , which is accepted to be equal to U_{mf} at low fluidizing velocity. Rigorously, the superficial gas velocity in the emulsion phase must be calculated using a gas volumetric flow balance leading to the expression $U_{1e} = (U_f - \delta\varepsilon_b U_b)/(1 - \delta)$, and the variables are experimental data integrated on the whole fluidized bed section. Thus, the superficial gas velocity in the emulsion-phase remains constant and closed to U_{mf} when the fluidizing velocity is lower than U_c , (Fig. 10). Nevertheless, the superficial gas velocity in the emulsion-phase exponentially increases for higher fluidizing velocities, reaching twice the fluidizing velocity value, and the model assumptions are then not acceptable.

The increase in the superficial gas velocity in the emulsion-phase leads to modifications in bubble behavior through the fluidizing regimes. Indeed, the ratio of the interstitial gas velocity in the bubble- and emulsion- phases, $U_b/(U_{1e}/\varepsilon_e)$, shows that (Fig. 11) (i) bubbles are fast bubbles ($U_b/(U_{1e}/\varepsilon_e) \approx 4$) when fluidizing velocity ranges between U_{mf} and U_c , (ii) bubbles evolve from fast bubbles to emulsion-bubble equilibrium state ($U_b/(U_{1e}/\varepsilon_e) \approx 1$) when fluidizing velocity increases from U_c to U_c (iii) bubbles evolve from emulsion-bubble equilibrium state to slow bubbles ($U_b/(U_{1e}/\varepsilon_e) \approx 0.5$) above U_c . Finally, the importance of U_c is also illustrated with the fraction of the total gas mass flux through the bubble-phase (Fig. 12). While the empirical correlations and the classic

description of the bubbling phenomena show an increase in this value when increasing fluidizing velocity, experiments show that a maximum of gas travels in the bubble-phase around $U_{c'}$, and that the total fraction of gas in bubbles, $\delta \varepsilon_b U_b / U_f$, never exceeds 75-80 %. Furthermore, the total fraction of gas in bubbles remains constant when fluidizing velocity is increased above $U_{c'}$.

THEORETICAL DETERMINATION OF $U_{c'}$ AND CONSEQUENCES

Davidson-Harrison's modeling supplemented with the maximum fraction of gas criterion of 75-80 % through the bubble –phase leads to the estimation of $U_{c'}$ for any B-particle :

$$\begin{cases} \delta \varepsilon_b U_b / U_{c'} < 0.75 - 0.8 \\ \delta = (U_{c'} - U_{mf}) / U_b \\ U_b = U_{c'} - U_{mf} + 0.711 \sqrt{g \cdot d_b} \end{cases}$$

Results are plotted in Fig. 13. Largest B-particles ($U_{mf} \approx 0.25$ m/s, i.e. $d_p \approx 550$ μm and $\rho_p \approx 2500$ kg/m^3) exhibit a $U_{c'}$ equal to the transition criterion U_c . At the opposite, smallest B-particles ($U_{mf} \approx 0.01$ m/s, i.e. $d_p \approx 100$ μm and $\rho_p \approx 2500$ kg/m^3) exhibit a $U_{c'}$ closed to the minimum bubbling velocity of the biggest A-particles. Thus, $U_{c'}$ is a criterion of particle aerability. It introduces a new description of the B-particle fluidization : (i) when fluidizing velocity is well below $U_{c'}$, fluidized beds are strongly emulsion-aerated, and bed aeration from the bubble-phase is low (ii) when increasing the fluidizing velocity, bed aeration from the bubble-phase increases while bed aeration from the emulsion-phase decreases (iii) when fluidizing velocity reaches $U_{c'}$, aeration from the bubble-phase is maximum while bed aeration from the emulsion is minimum ; increasing

the fluidizing velocity above U_c , does not change the bed aeration rate from the emulsion- and the bubble- phases.

CONCLUSIONS

Extensive experiments are performed to investigate the transition between bubbling and turbulent regimes in the fluidized bed using pressure and bi-optical probes.

First, standard data are provided to characterize the fluidized bed hydrodynamics : (i) time-averaged local pressure drops (ii) time-averaged values, standard deviations, probability density function distributions, dominant frequencies of the local voidage fluctuations (iii) time-averaged bubble chords and velocities, bubbling frequency.

Second, extra data are provided to improve our understanding of the bubbling phenomena : (i) interstitial gas velocity of the emulsion-phase (ii) fraction of the total gas mass flux through the bubble-phase.

No peculiar phenomenon suddenly appears or disappears at gas velocity transition criterion, U_c , determined based on pressure fluctuations. A peculiar velocity, U_c' , is a more critical parameter in the bubbling to fast fluidization regime transition. Indeed, we observe that : (i) standard two-phase modeling assumptions are acceptable for fluidizing velocities lower than U_c' ; they are not acceptable for higher fluidizing velocities, and the model leads to partial slanted predictions for higher fluidizing velocity (ii) the fraction of total gas mass flux through the bubble-phase reaches a maximum value at U_c' , and never exceeds 75-80 % ; it remains constant above U_c' (iii) bubbles are fast bubbles below

U_c' ; bubbles evolve to emulsion-bubble equilibrium state when fluidizing velocity reaches U_c' ; bubbles are low bubbles when increasing the fluidizing velocity.

Moreover, U_c' is equal to U_c for biggest B-particles and is of the same order of magnitude than the minimum bubbling velocity of A-particles for smallest B-particles. Thus, U_c' is a criterion of particle aerability.

U_c' could be determined either by the break point in the pressure drop curve, or by the maximum of the local voidage dominant frequency, both observed when increasing fluidizing velocity from U_{mf} to U_c' . It can also be determined theoretically using the criterion of maximum fraction of gas in the bubble-phase, equal to 75-80 %.

ACKNOWLEDGEMENTS

The authors would like to acknowledge the Institut Français du Pétrole (IFP) for its financial support and for providing the possibility of post-graduate studies for Dr. Régis Andreux, and the Institut de Mécanique des Fluides de Toulouse, France, for its computational support. Many thanks to Pierre Sauriol, from the Chemical Engineering Dpt. of Ecole Polytechnique de Montréal , for all the help and technical assistance he provided us during the present work, and to Heping Cui for providing the optical probe.

LIST OF NOTATION

Roman letters

Ar Archimedes number (-)

d_b	Mean bubble chord (m)
d_p	Particle phase mean diameter (m)
g	Gravity (m^2/s)
U_b	Mean bubble velocity (m)
U_c	Transition criterion determined based on the pressure fluctuations (m/s)
$U_{c'}$	Transition criterion determined based on the break point of ΔP curve (m/s)
U_f	Fluidizing velocity (m)
U_{1e}	Superficial gas velocity in the emulsion-phase (m/s)
U_{mf}	Minimum fluidizing velocity (m/s)

Greek letters

δ	Void-phase fraction in the two-phase modeling formalism (-)
ε_k	Voidage of phase k in the two-phase modeling formalism (-)
ε_f	Local bed voidage (-)
ε_{mf}	Bed voidage at minimum fluidizing velocity (-)
μ_1	Fluid dynamic laminar viscosity (Pa s)
ρ	Density (kg/m^3)

Subscripts

b	Bubble phase in the two-phase modeling formalism
e	Emulsion phase in the two-phase modeling formalism

REFERENCES

1. Lanneau KP. Gas-Solid Contacting in Fluidized Beds. Trans. Inst. Chem. Eng. 1960 ; 38 : 125-137.
2. Horio M, Ishii H, Nishimuro M. On the Nature of Turbulent and Fast Fluidized Beds. Powder Techn. 1992 ; 70(3) : 229-236.
3. Rhodes M. What is Turbulent Fluidization ? Powder Techn. 1996 ; 88 : 3-14.
4. Bi HT, Ellis N, Abba IA, Grace JR. A State-of-the-Art Review of Gas-Solid Turbulent Fluidization. Chem.Eng. Sc. 2000 ; 55 : 4789-4825.
5. Tannous K, Hemati M, Laguerie C. Identification of Flow Regime Transitions in Fluidized Beds of Large Particles by Pressure Drop Fluctuation Measurements. Brazilian J. of Chem. Eng. 1996 ; 13(3) : 168-181.
6. Bai D, Shibuya E, Nakagawa N, Kato K. Characterization of Gas Fluidization Regimes using Pressure Fluctuations. Powder Techn. 1996 ; 87 : 105-111.
7. Makkawi YT, Wright PC. Fluidization Regimes In A Conventional Fluidized Bed Characterized By Means Of Electrical Capacitance Tomography. Chem. Eng. Sc. 2002 ; 57 : 2411-2437.
8. Svensson A, Johnsson F, Leckner B. Fluidization Regimes In Non-Slugging Fluidized Beds : The Influence of Pressure Drop Across the Air Distributor. Powder Techn. 1996 ; 86(3) : 299-312.
9. Yamazaki R, Asai M, Nakajima M, Jimbo G. Characteristics of Transition Regime in a Turbulent Fluidized Bed. In : 4th China-Japan Fluidization Conference Proc., Beijing Sc. Press. 1991 : 720-725.

10. Zijerveld RC, Johnsson F, Marzocchella A, Shouten JC, Van Den Bleek CM. Fluidization Regimes And Transitions From Fixed Bed To Dilute Transport Flow. Powder Techn. 1998 ; 95(3) : 185-204.
11. Xie H-Y, Geldart D. The Response Time of Pressure Probes. Powder Techn. 1997 ; 90 : 149-151.
12. Cui H, Mostoufi N, Chaouki J. Characterization of Dynamic Gas-Solid Distribution in Fluidized Beds. Powder Techn. 2000 ; 79 : 133-143.
13. Bayle J, Mege P, Gauthier T. Dispersion of Bubble Flow Properties in a Turbulent FCC Fluidized Bed. In : Fluidization X – 10th Engineering Foundation Conference. Beijing, Proceedings, Kwauk M et al. Eds., 2001 : 125-132.
14. Gonzalez A, Chaouki J, Chehbouni A. Effect of Temperature on the Onset of Turbulent Fluidization. In : Fluidization VIII – 8th International Symposium Of the Engineering Foundation, Tours, France. 1995.
15. Bi HT, Grace JR. Flow Regime Diagrams For Gas-Solids Fluidization and Upward Transport. Int. J. Multiphase Flows. 1995 ; 21 : 1229-1236.
16. Abba IA. A Generalized Fluidized Bed Reactor Model across the Flow Regimes. PhD Thesis, University of British Columbia, Vancouver, Canada. 2001.
17. Lancia A, Nigro R, Volpicelli G, Santoro L. transition from Suggling to Turbulent Flow Regimes in Fluidized Beds Detected by Means of Capacitance Probes. Powder Techn. 1988 ; 56(1) : 49-56.
18. Cui H, Mostoufi N, Chaouki J. Gas and Solids between Dynamic Bubble and Emulsion in Gas-Fluidized Beds. Powder Techn. 2001 ;120 : 12-20.

19. Darton RC, Lanauze RD, Davidson JF, Harrison D. Bubble Growth due to Coalescence in Fluidized Beds. *Trans. Inst. Chem. Eng.* 1977 ; 55 : 274-280.
20. Davidson JF, Harrison D. *Fluidized Particles*. Cambridge University Press. 1963.
21. Ergun S. Fluid Flow Throught Packed Columns. *Chem. Engng Progr.* 1952 ; 48 : 89-94.
22. Grace JR. *Handbook of Multiphase Systems*. G. Hestroni ed., Hemisphere, Washington, D.C. 1982.

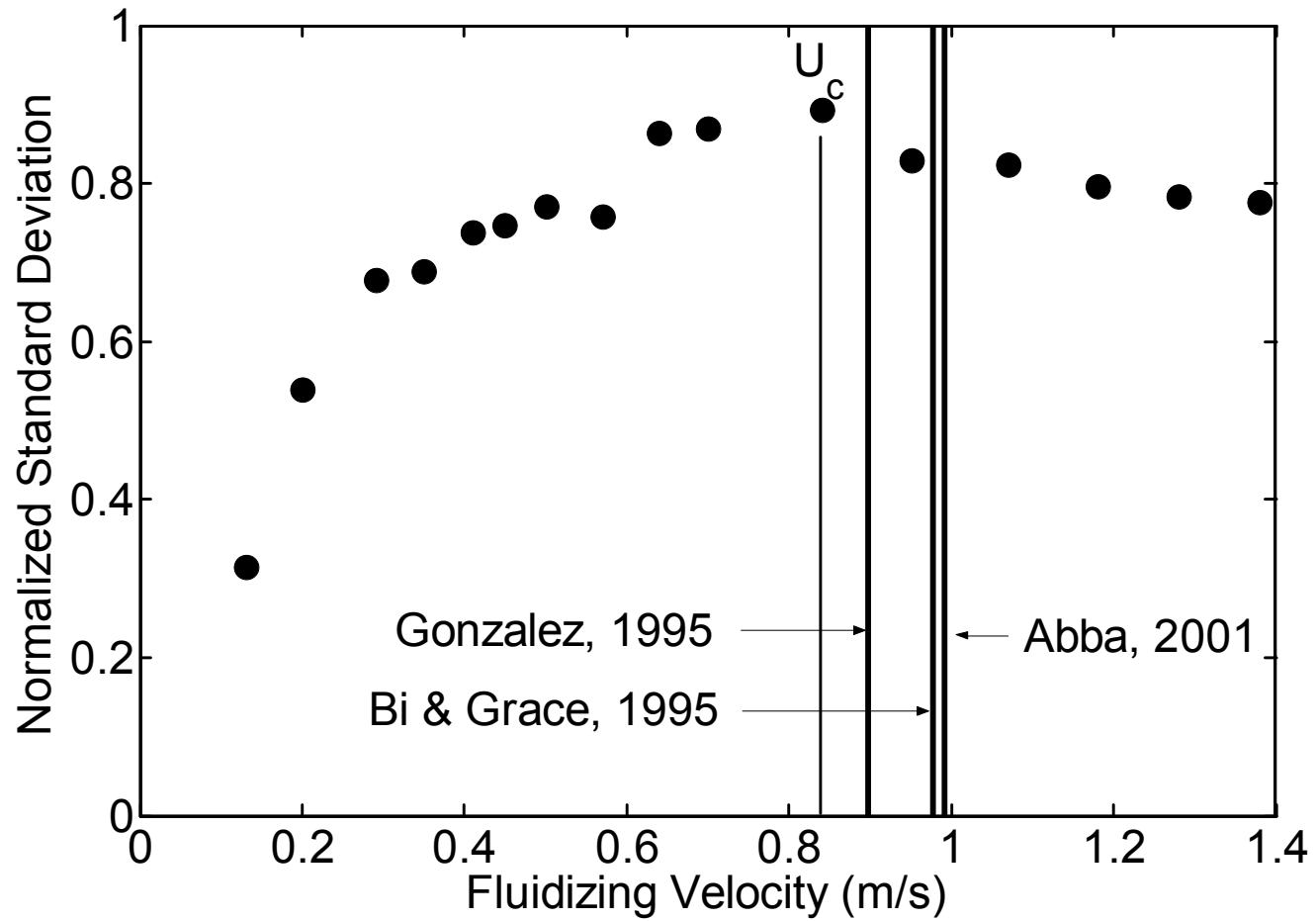


Figure 1: Experimental determination of the transition criterion U_c determined based on pressure fluctuations.

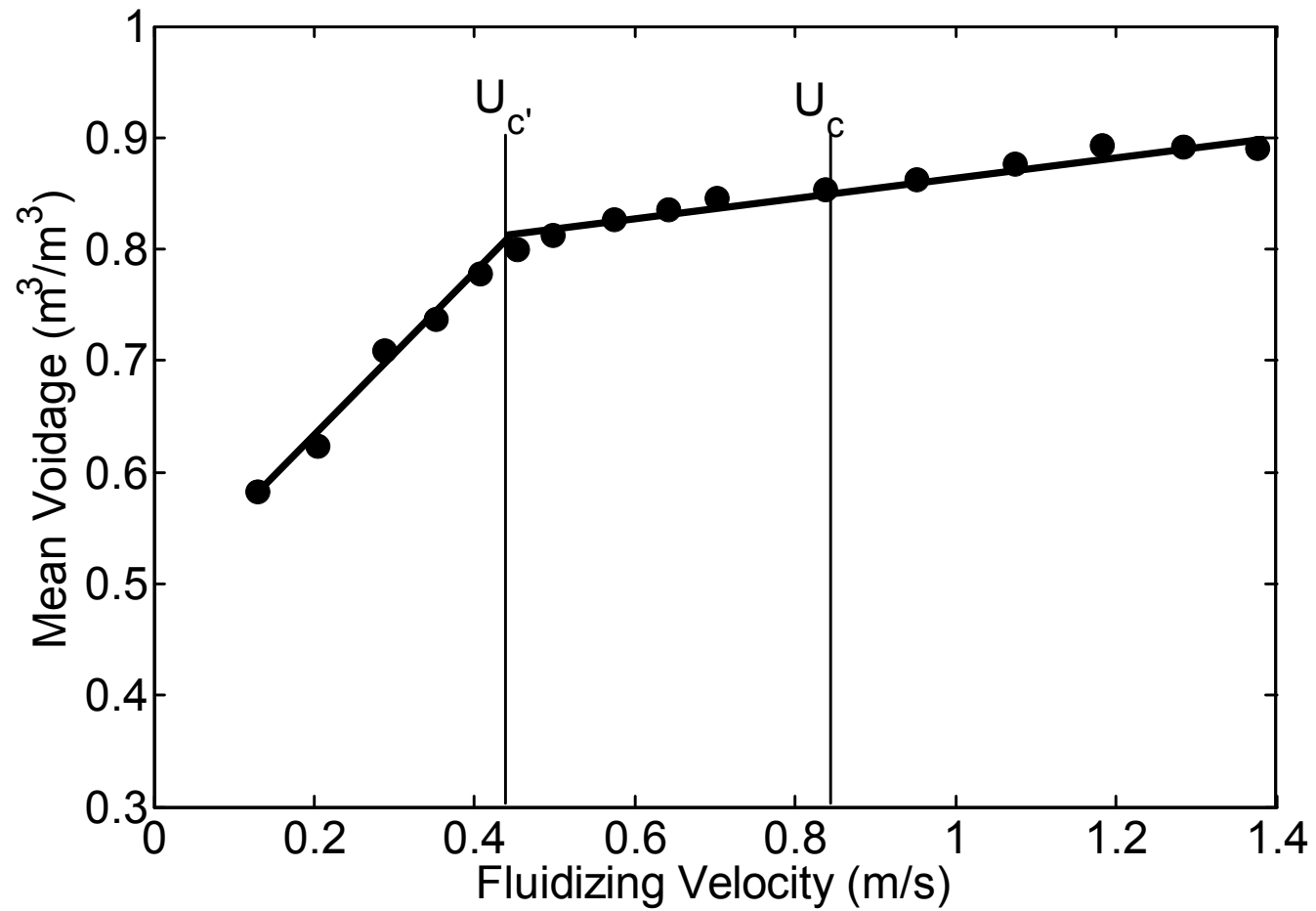


Figure 2: Time-averaged voidage at 30 cm above the distributor, determined based on the local pressure drop.

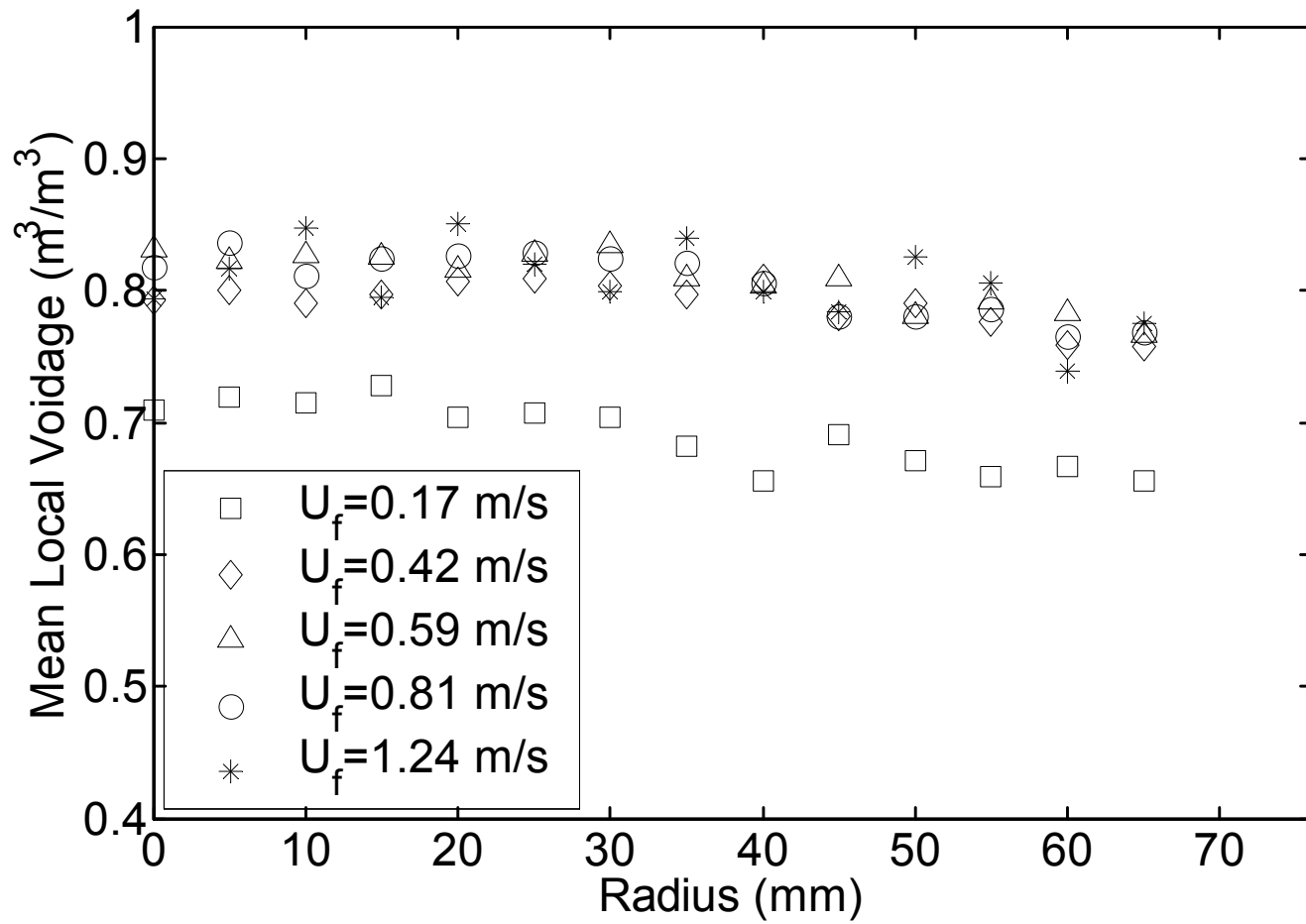


Figure 3: Time-averaged profiles of the local voidage at 30 cm above the distributor.

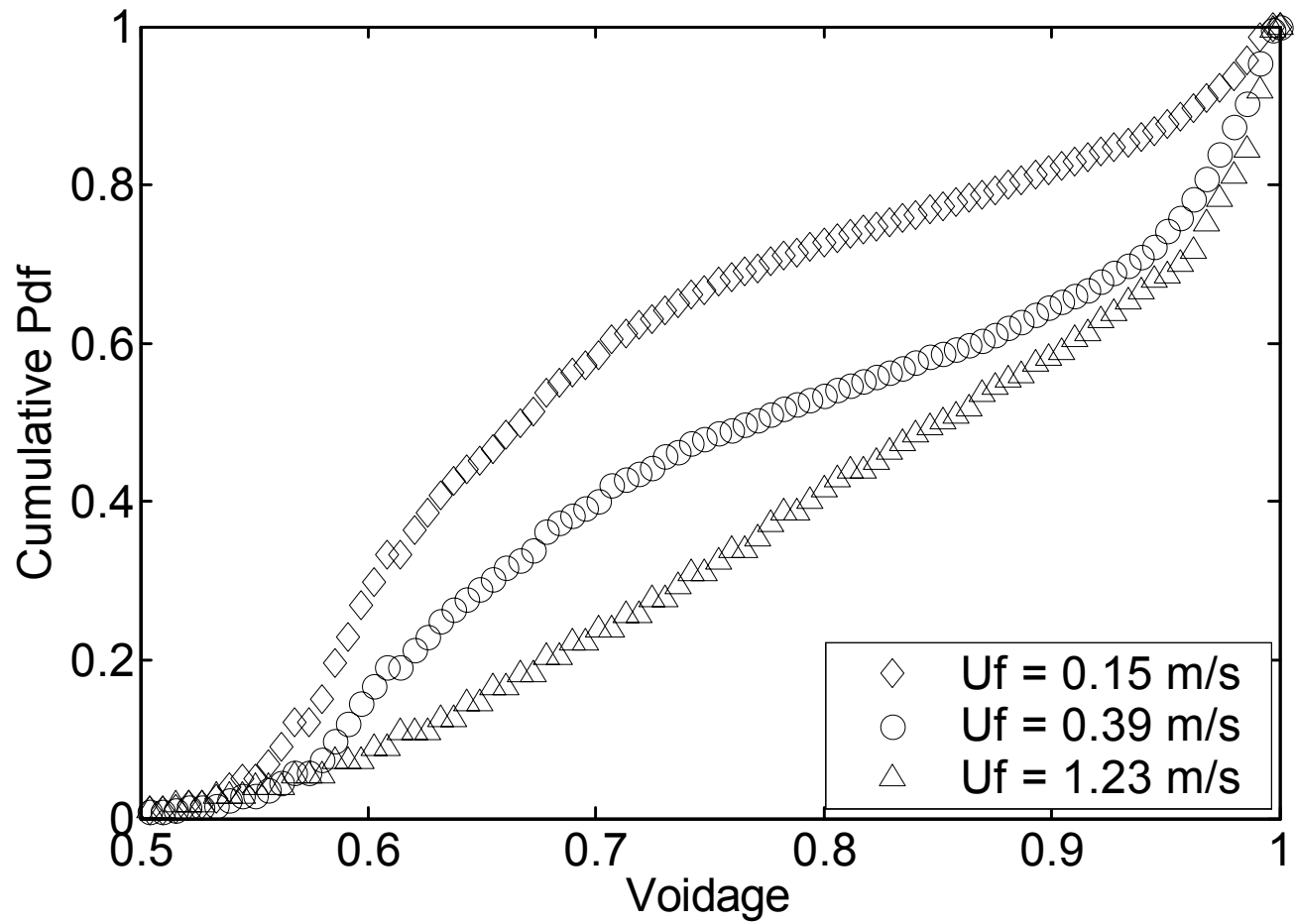


Figure 4: Cumulative probability density function of the local voidage at the centre of the bed and 30 cm above the distributor.

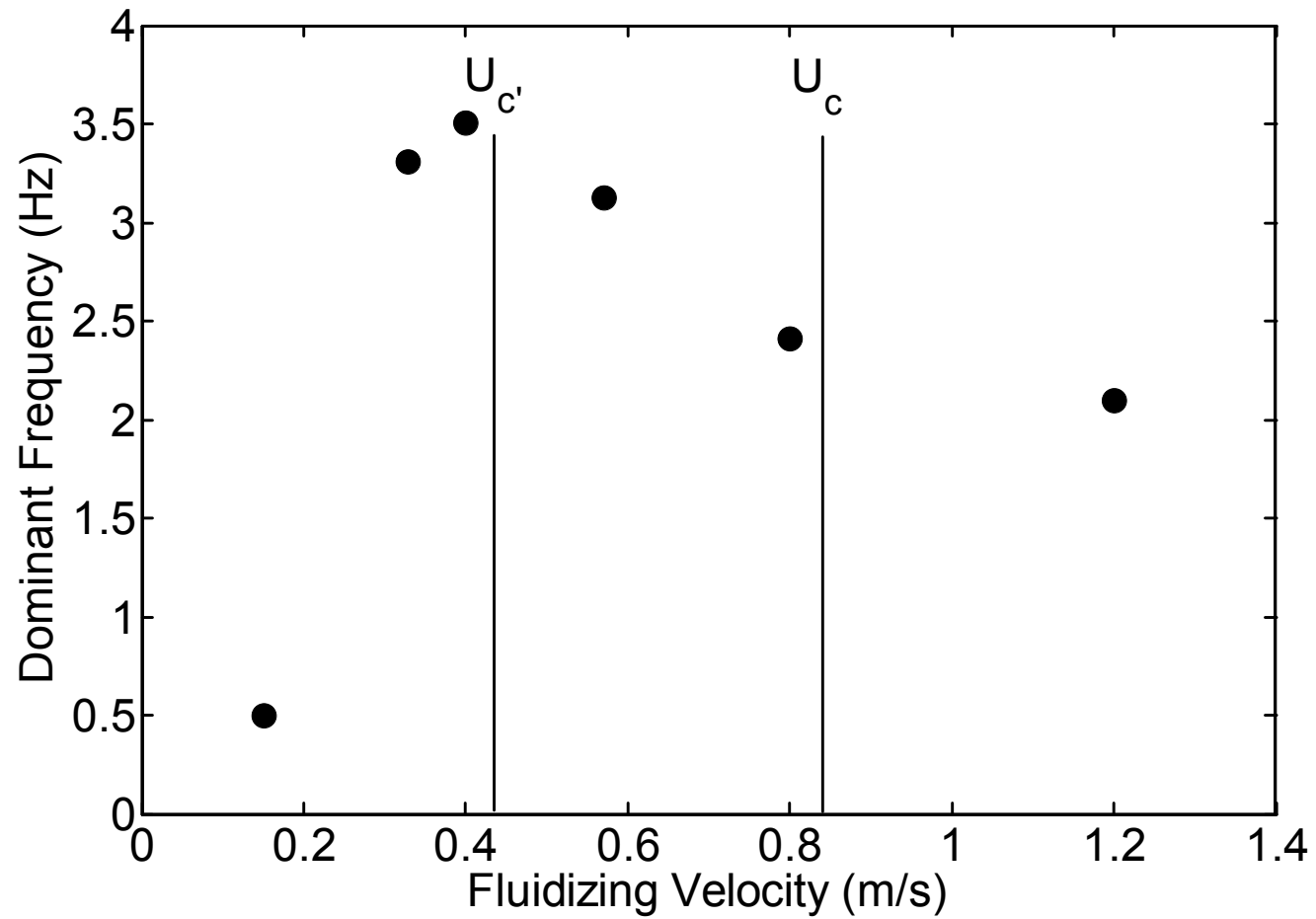


Figure 5: Dominant frequency of the local voidage at the centre of the bed and 30 cm above the distributor.

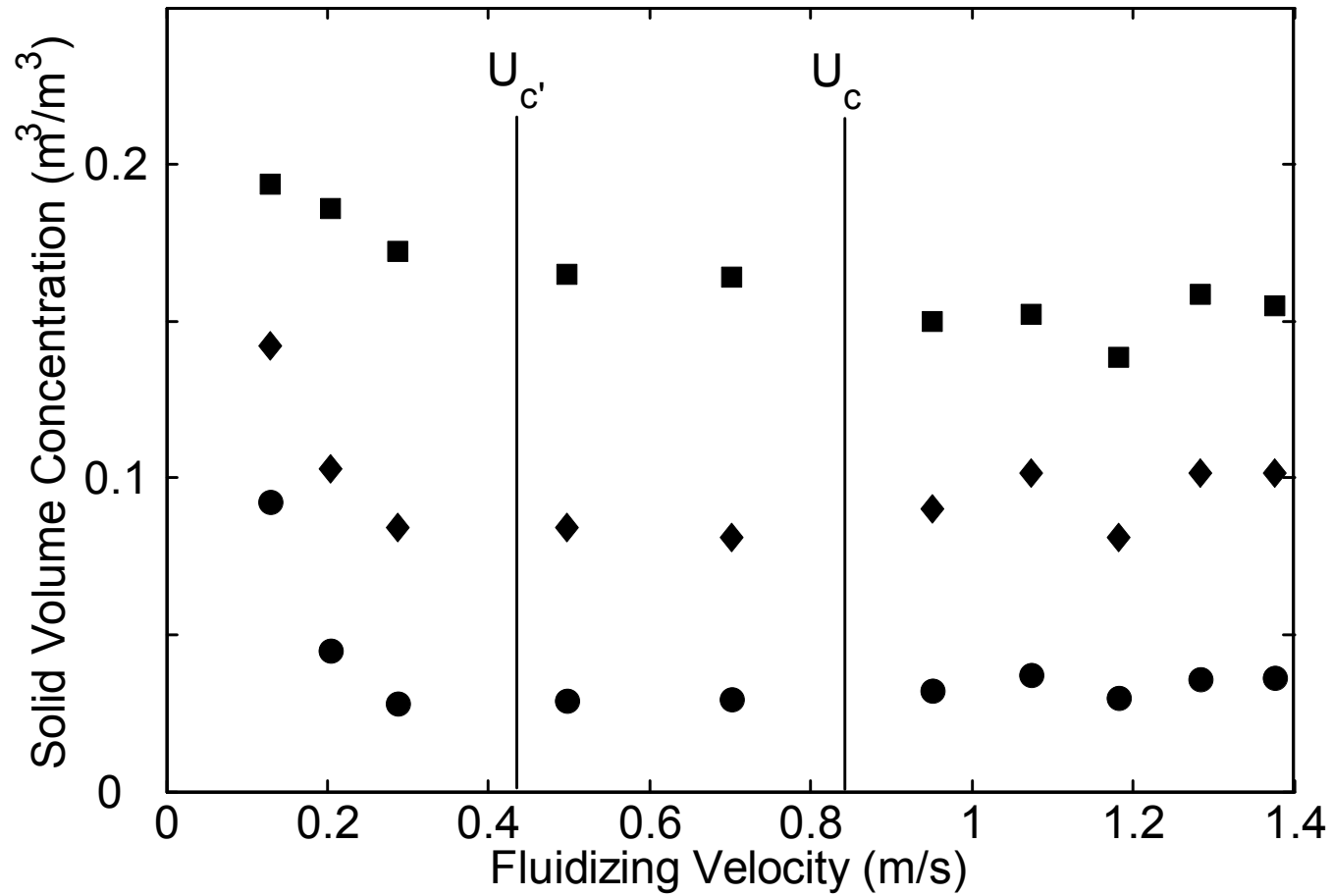


Figure 6: Solid volume concentration threshold, \diamond , of the bubble-, \circ , and the emulsion-phase, \square , at the centre of the bed and 30 cm above the distributor.

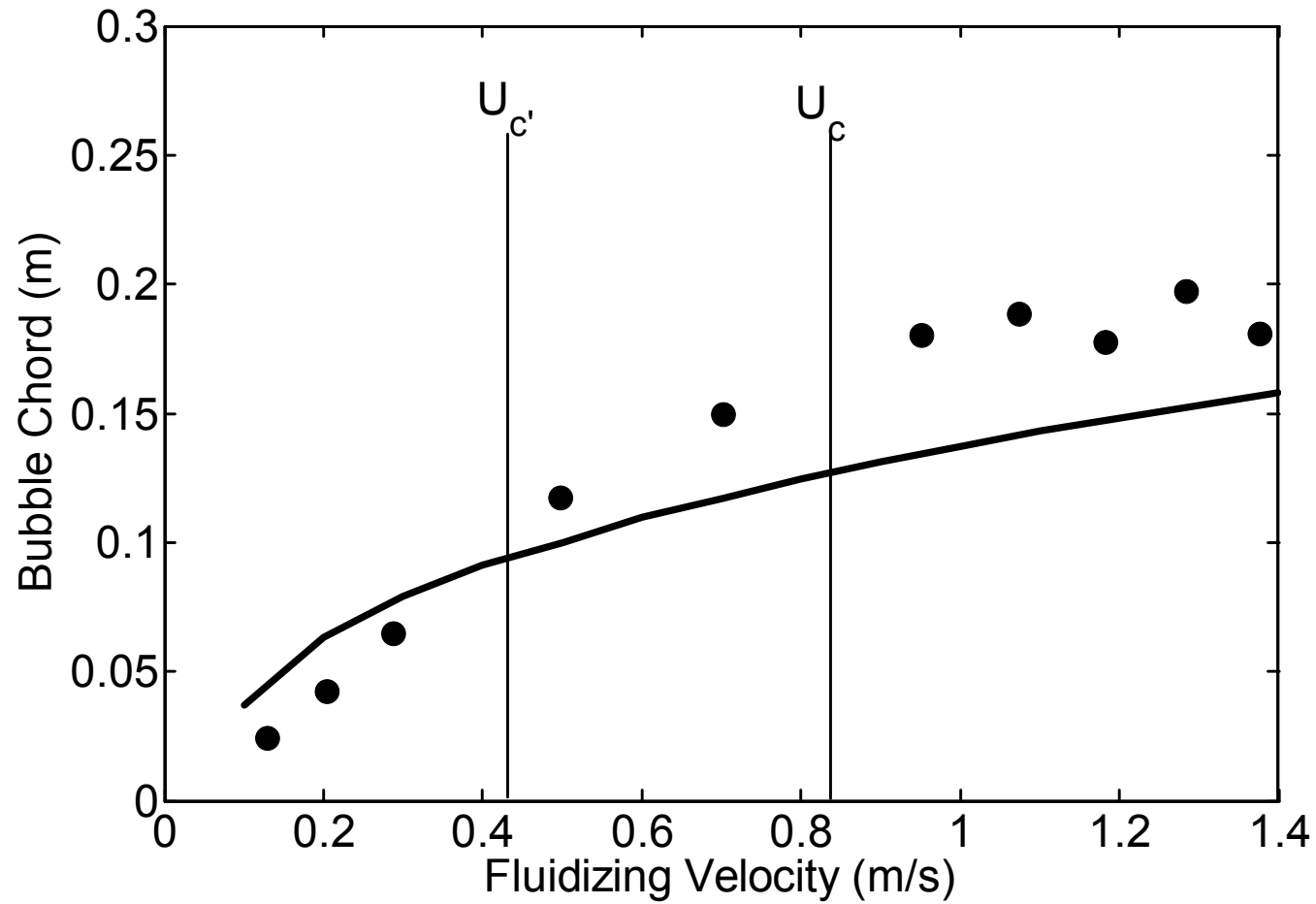


Figure 7: Time-averaged bubble chord at the centre of the bed and 30 cm above the distributor (● : experiments ; — : Two-phase modeling).

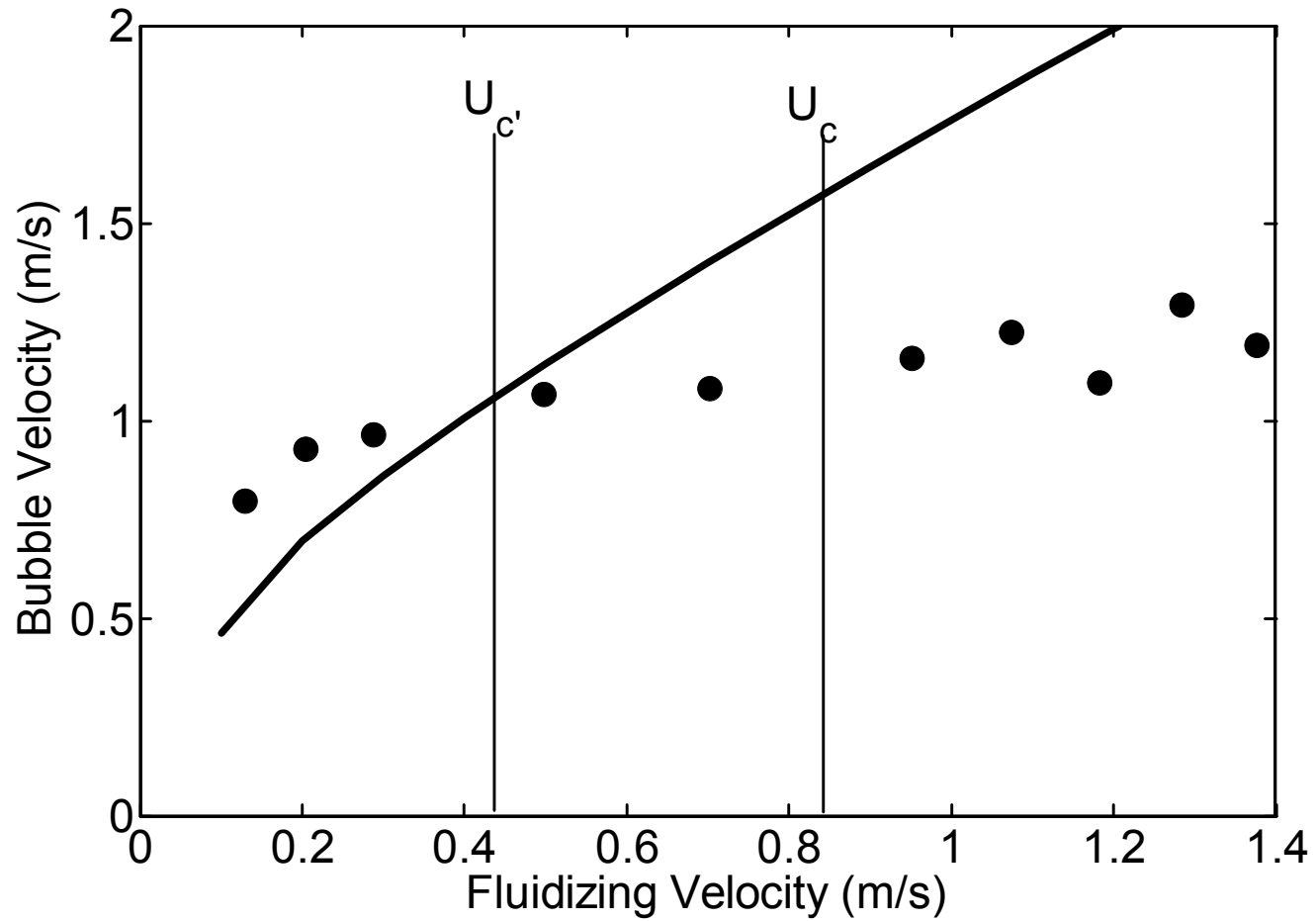


Figure 8: Time-averaged bubble velocity at the centre of the bed and 30 cm above the distributor (● : experiments ; — : Two-phase modeling).

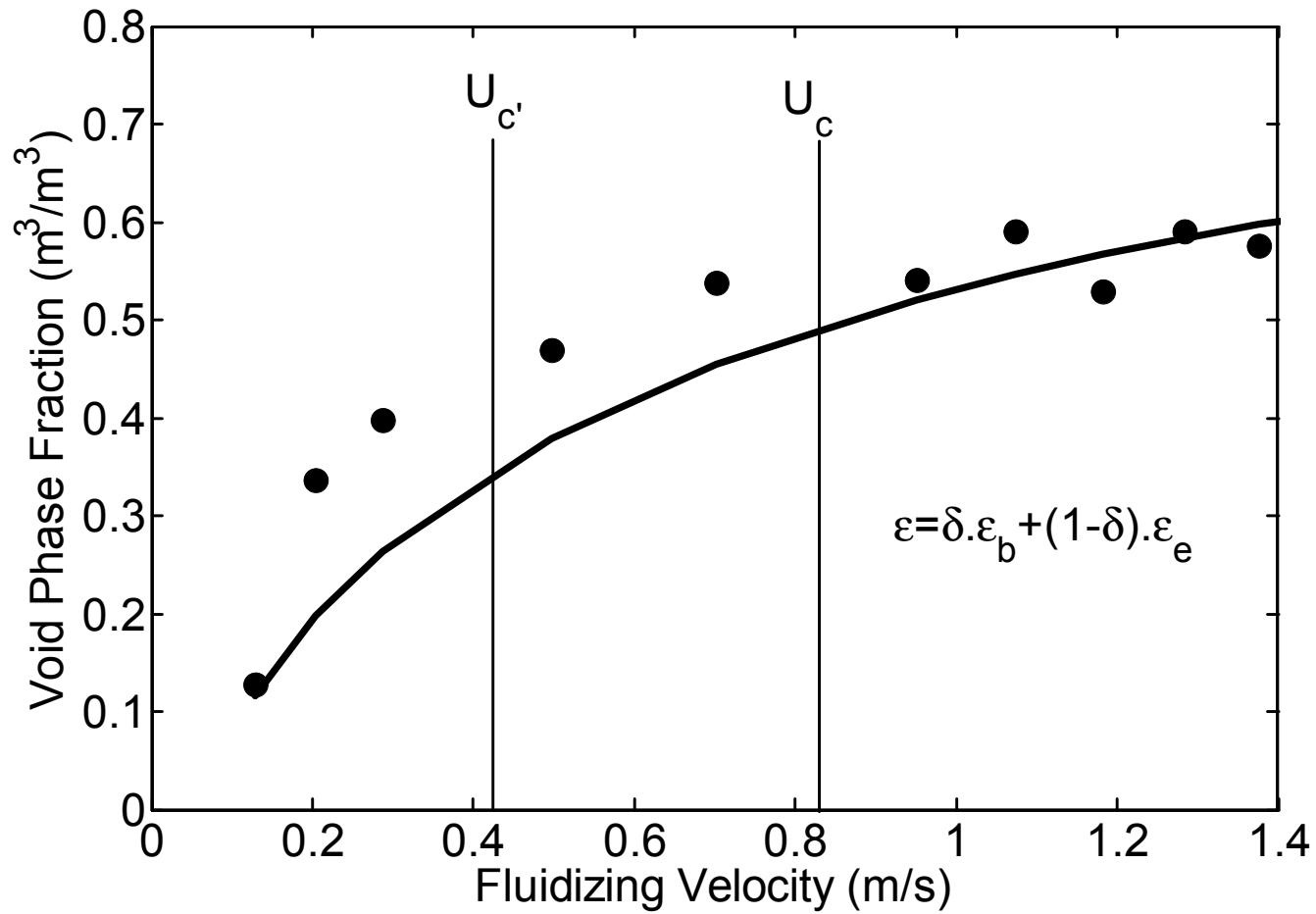


Figure 9: Void-phase fraction at the centre of the bed and 30 cm above the distributor (● : experiments ; — : Two-phase modeling).

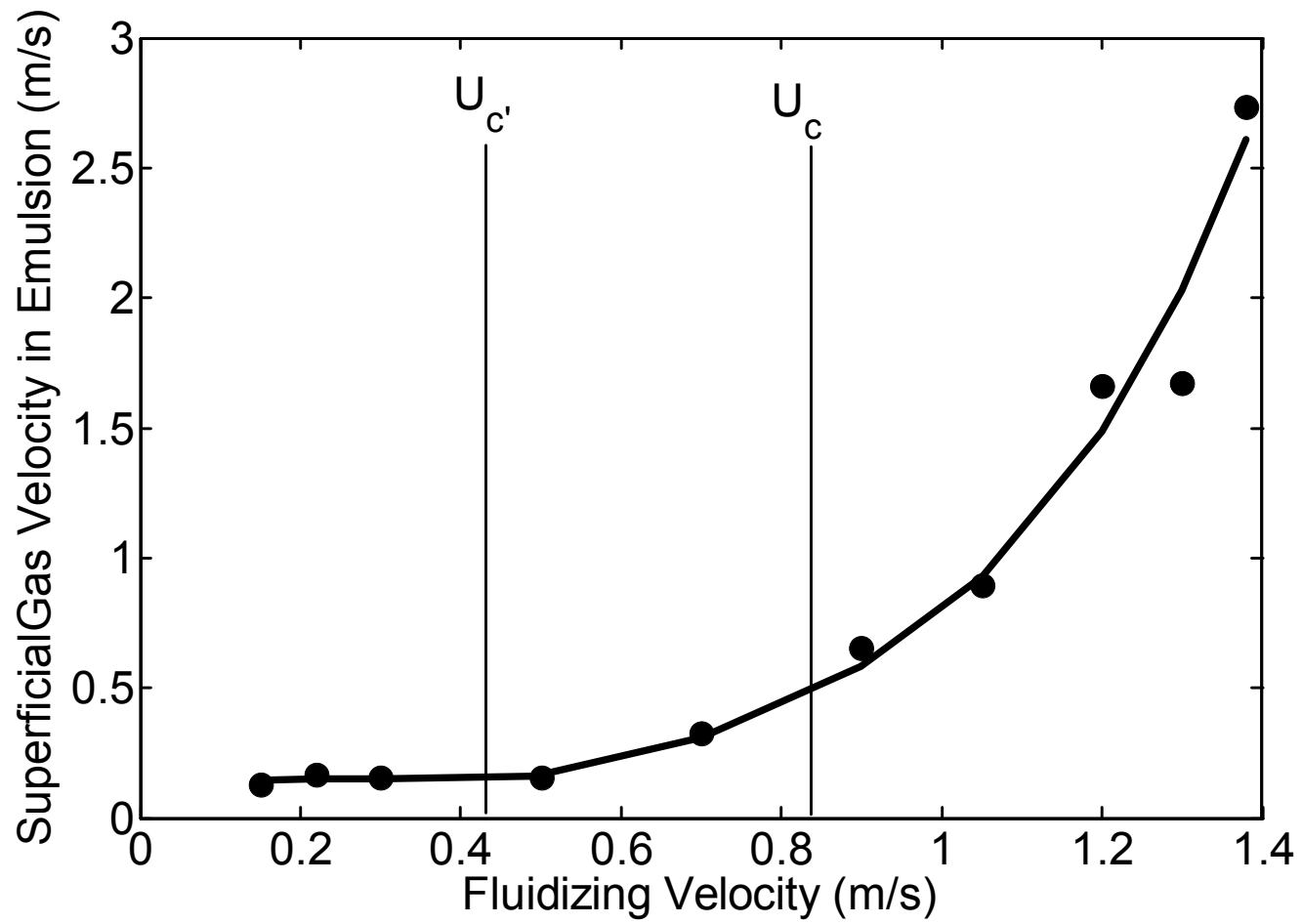


Figure 10: Experimental superficial gas velocity in the emulsion-phase.

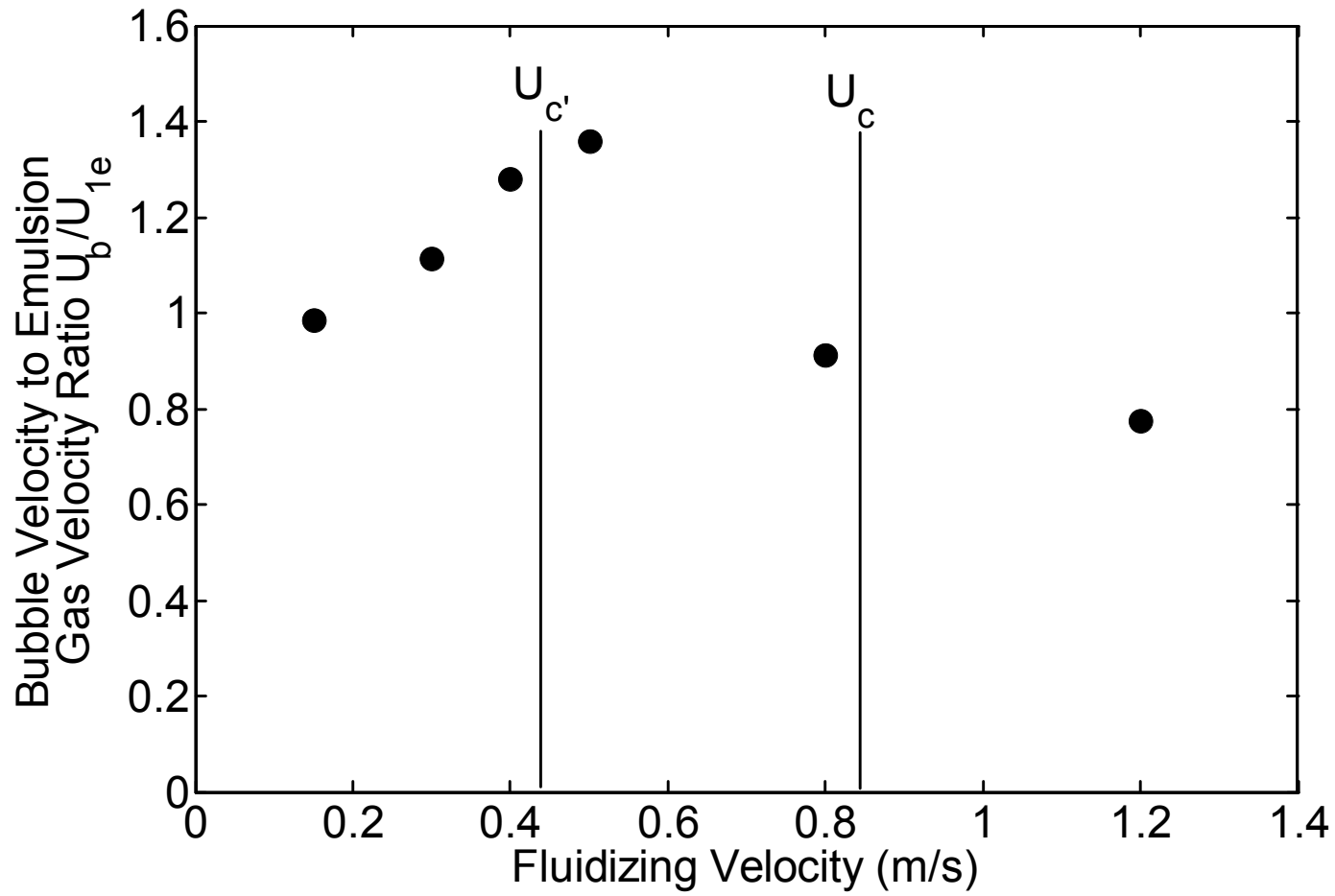


Figure 11: Bubble velocity to interstitial gas velocity in the emulsion ratio.

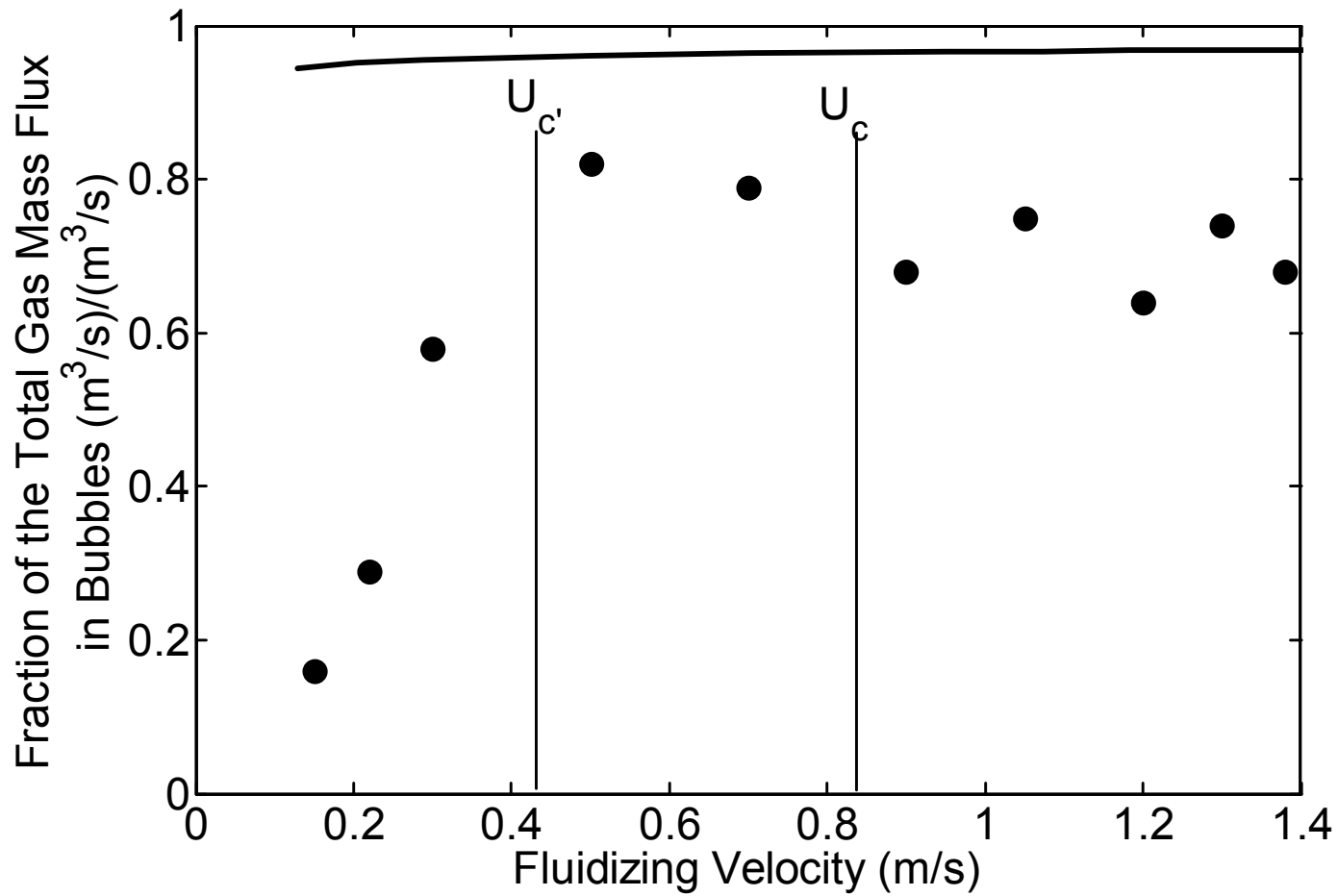


Figure 12: Fraction of the total gas mass flux in the bubble-phase (● : experiments ; — : Two-phase modeling).

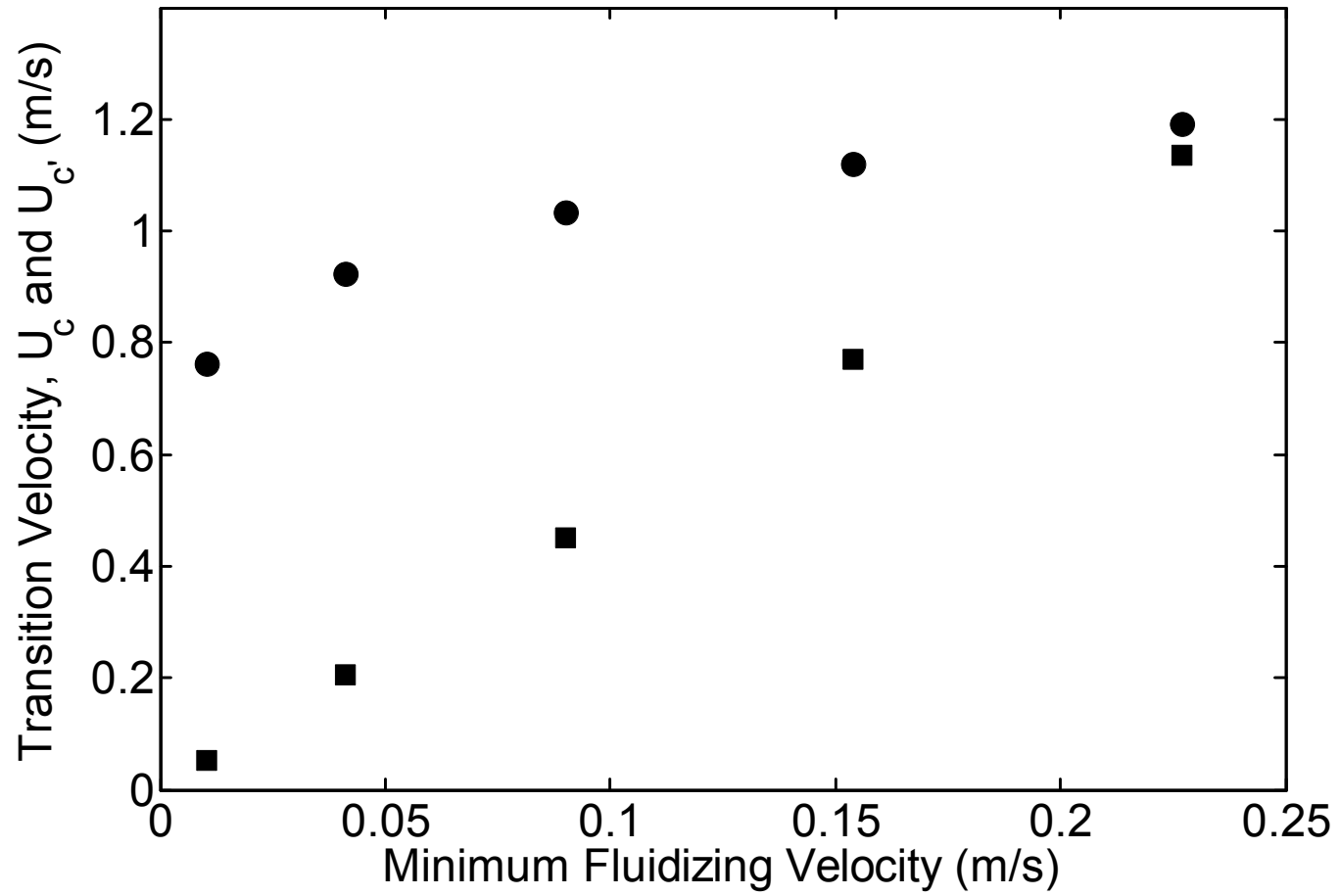


Figure 13: Transition criterion velocity (\bullet : U_c ; \blacksquare : $U_{c'}$).